Simulation and Prediction of Cardiotherapeutical Phenomena From a Pulsatile Model Coupled to the Guyton Circulatory Model

Jürgen Werner*, Daniel Böhringer, and Martin Hexamer

***Abstract*—In order to use simulation prediction for cardiotherapeutical purposes, the well-documented and physiologically validated circulatory Guyton model was coupled to a cardiac pulsatile model which comprises the hemodynamics of the four chambers including valvular effects, as well as the Hill, Frank–Starling, Laplace, and autonomic nervous system (ANS) effects. The program is written in the "C" language and available for everybody.**

The program system was submitted to validation and plausibility tests both as to the steady-state and the dynamic properties. Pressures, volumes and flows and other variables turned out to be compatible with published experimental and clinical recordings both under physiological and pathophysiological conditions. The results from the application to cardiac electrotherapy emphasize the importance of atrial contraction to ventricular filling, the adequate atrio-ventricular delay, the effect of impaired ventricular relaxation, and the significance of the choice of the adequate cardiac pacemaker, both with respect to the stimulation site and the adequate sensor controlling pacing rate. The simulation will be further developed, tested and applied for cardiological purposes.

***Index Terms*—Cardiotherapy, cardiovascular model, electrotherapy, hemo-dynamics, pulsatile processes, relaxation disorder.**

I. Introduction

THE list of cardio-circulatory models is almost infinite, with manifold reasons for such an abundance. On the one hand, engineering and computing possibilities are continually increasing, on the other hand the physiological insight in the functional processes is growing at a great rate. Furthermore, the general guideline of modeling holds that the complexity and the properties of a model should be adapted to the purpose of the model, which makes clear that we will never have the general purpose model. From the methodological aspect we have mainly early analog computer models (e.g., [1]–[3]), which in many cases were transferred to digital simulation languages (e.g., CSMP, SIMULINK), others were written in conventional digital programming languages (e.g., [4]) or even handled by computer-aided design packages [5].

Many have proved their usefulness in education and training (e.g., [6]–[8]), others were mainly developed to contribute to special scientific problems, such as left-ventricular pumping function [9], orthostasis [10], pulmonary circulation [11], vasodilatation therapy [12], [13], or flow velocity patterns [14].

Generally speaking, the published models are optimized for either studying short term mechanics of blood circulation and myocardial performance: pulsatile models, e.g., [15], or mid- and long-term regulatory effects such as exercise, homeostasis, and metabolism; regulatory models, e.g., [3]. The model with the most comprehensive physiological background is the "large Guyton model," first published in 1972 [3] and continuously modified and complemented by the authors (e.g., [16]–[18]), however, it does not consider the beat-to-beat processes crucial to the analysis of regulatory effects within the heart.

Therefore, in order to save the enormous knowledge and experience of the Guyton model and to make use of them in wider applications, we decided to couple a pulsatile model with the Guyton model. To do this we first had to develop a pulsatile component which could functionally substitute the nonpulsatile "circulatory dynamics" component of the Guyton model. The motivation for this was the need to develop predictive criteria for the short- and long-term effects of cardiotherapeutical treatments. After general validation and tests of plausibility of physiological and pathophysiological phenomena, we first used the coupled system to compute and to predict various effects of electrotherapy, such as the importance of atrial stimulation (versus or in combination with ventricular stimulation), of an adequate atrioventricular delay and a characterization and optimization of sensor-controlled (rate-adaptive) pacing.

II. Materials and Methods

A. Overview on the Guyton Model

The Guyton model is well documented and based on physiological knowledge, parameters and validation ([3], [16]–[18]). Therefore we will give only a short overview (Fig. 1). Strictly speaking it consists of 17 modules containing about 600 physiological parameters and variables. It was originally written in FORTRAN, but was later translated into "C" by Guyton and his colleagues [18]. The kernel of the model is the "circulatory dynamics" module, which we substituted by a pulsatile model to be outlined in more detail below. The other modules were only modified to a low extent. The module "Autonomics" refers to control of cardiocirculation via arterial baroreceptors, peripheral and central chemoreceptors, and ergoreceptors (physical exercise). In view of coupling it to the pulsatile module, we had to include an adequate dynamic activation of signals from

Manuscript received June 22, 2001; revised December 19, 2001. This work was supported by Deutsche Forschungsgemeinschaft under Grant We 919/16-1. *Asterisk indicates corresponding author*.

*J. Werner is with the Department of Biomedical Engineering of the Medical Faculty, Ruhr-University, MA 4/59, D-44780 Bochum, Germany (e-mail: werner@biomed.ruhr-uni-bochum.de).

D. Böhringer and M. Hexamer are with the Department of Biomedical Engineering of the Medical Faculty, Ruhr-University, D-44780 Bochum, Germany.

Publisher Item Identifier S 0018-9294(02)03999-X.

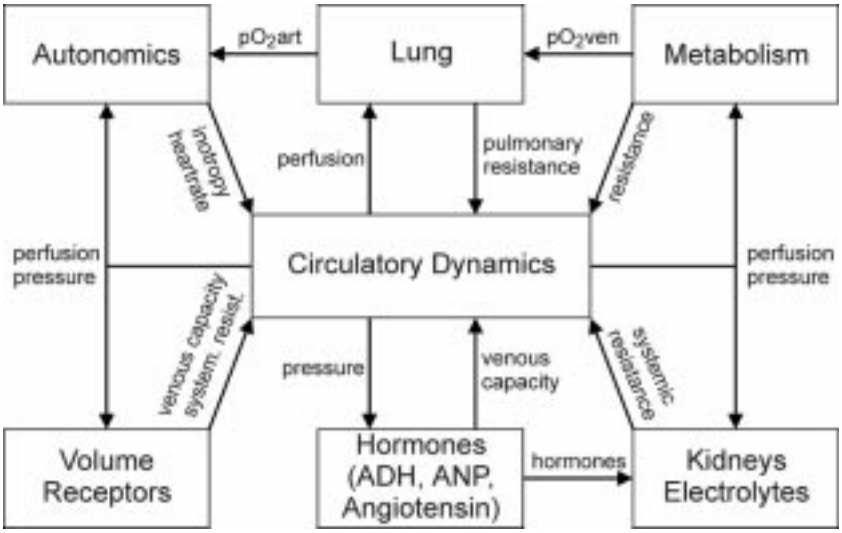

Fig. 1. Simplified structure of the large Guyton model. [3], [16]–[18] A new (pulsatile) module "Circulatory Dynamics" (see Fig. 2) has been developed and coupled to the Guyton model (pO_2 = oxygen partial pressure).

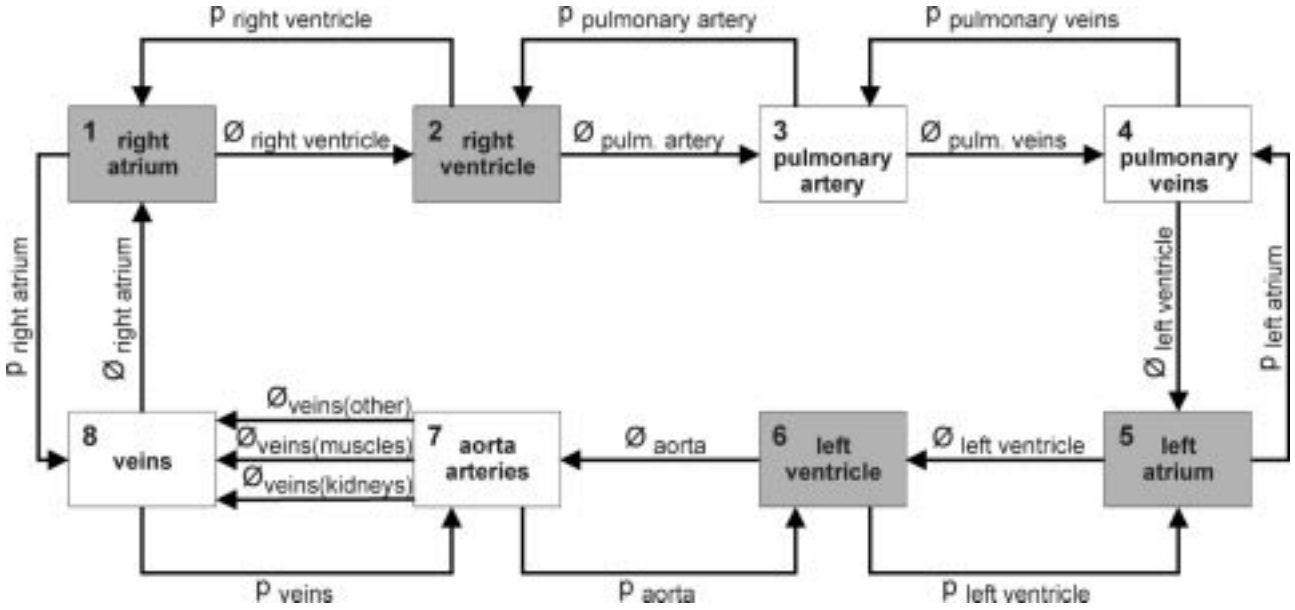

Fig. 2. Survey on the pulsatile cardiocirculatory model ($\varnothing$ = flow, p = pressure).

the autonomic nervous system (ANS). "Volume receptors" take into account the effect of the right-atrial volume on the venous tone and the arterial resistance. The block "metabolism" summarizes oxygen delivery to muscle and nonmuscle tissue, and local blood flow control (short-term via hypoxia-mediated vasodilatation, mid-term via tissue mediators, and long-term via structured tissue changes). The "lung" module mainly simulates the oxygen binding process in the erythrocytes. Further modules comprise hormonal, renal, and electrophysiological processes.

B. Pulsatile Model

In the pulsatile model, blood circulation is represented by linked compartments with the attributes volume, pressure, inflow, and outflow (see Fig. 2 for a synopsis of the compartments and their interdependencies). The hemodynamic beat-to-beat changes are implemented by exclusively varying the wall tension of the ventricles and of the atria over a period of time, with all other variables resulting from the physics of fluid mechanics.

The reason for exactly modeling the compartments as shown in Fig. 2 is the necessary compatibility with the large circulatory model of Guyton. The cardiac output is split into muscular and renal, and the remaining part on its way from the systemic arteries to the veins. This facilitates simulation of exercise conditions where blood flow is redirected toward muscular tissue.

1) Physics of the Pulsatile Model: Inside the heart (highlighted compartments in Fig. 2), a volume pulse is forcefully accelerated in systole. Hence, this dynamic flow of blood has to be expressed in terms of the hydrostatic pressure gradient (Δp), the pressure drop due to viscosity induced friction ($R\Phi$),

and—the third term on the right side of (1)—the acceleration induced pressure drop

$$L\frac{d\Phi}{dt} = \Delta p - R\Phi - \frac{\rho}{2}\left(\nu_0^2 - \nu_1^2\right). \quad (1)$$

In (1), in order to work with commonly used amounts of pressures and flows, we use the units indicated in brackets: Δp [mm Hg] is the hydrostatic pressure gradient and Φ [l/min] is the flow between both compartments with initial velocity ν_0 and final velocity ν_1 [dm/min]. L [mm Hg min^2/l] is a constant derived from the geometry (see below), ρ [kg/l] is the density of blood, and R [mm Hg min/l] is the resistance to the flow in the geometry considered.

The constant L, the so called inertance, relates the pressure pulse to the volume pulse: the larger L is, the more the volume pulse lags the pressure pulse. In a nonelastic tube, L can be calculated the following way:

$$L = \frac{\rho l}{a}. \quad (2)$$

In (2), l [cm] is the length, a [cm^2] is the cross-sectional area, and ρ [kg/l] is the density of blood of the accelerated volume pulse.

Since the blood inside the heart is accelerated in a pulsatile fashion on the way through atria and ventricles, it has a negligible flow velocity most of the time. This is the reason for adopting the following simplified variant of (1) (note that the flow-velocity was substituted with the equivalent quotient of Φ [l/min] and area A [cm^2]):

$$L\frac{d\Phi}{dt} = \Delta p - R\Phi - \frac{\rho}{2}\left(\frac{\Phi}{A}\right)^2. \quad (3)$$

This approach of describing blood flow inside the heart is common to most pulsatile models of the heart function (see [19]).

For the mathematical description of the blood flow in all major systemic arteries, the impedance has to be taken into account in addition to the classic frictional resistance component. This is crucial, e.g., for the dip in the aortic pressure curve in early diastole to evolve [Fig. 5(a)]. The aortic impedance is modeled in a simplified fashion by linking three compartments with decreasing compliance. The compliance is defined as the first derivative of the pressure-volume relation of each segment. The blood flow through these compartments is calculated using (4), a variant of (3). The neglected term $(0.5\,\rho\,(\Phi/A)^2)$ does not influence the results under physiological conditions (less than 1 mm Hg)

$$L\frac{d\Phi}{dt} = \Delta p - R\Phi. \quad (4)$$

In all compartments outside the heart the blood flow is assumed to be laminar and, thus, a constant frictional resistance to blood flow is applied according to the Hagen-Poiseuille law

$$\Delta p = R\Phi. \quad (5)$$

In (5), R [mm Hg min/l] is the resistance to laminar flow, Φ [l/min] is the flow through the compartments under consideration, and Δp [mm Hg] is the pressure difference necessary for Φ.

The pressure in each compartment is a function of the intracompartmental volume. This function is either graphically defined using diagrams from the physiological textbooks, or linear for the venous compartments

$$p = \frac{V - V_0}{C}. \quad (6)$$

In (6), C [l/mm Hg] is the compliance, V [l] is the intracompartmental, and V_0 [l] is the unstressed volume.

In all compartments inflow and outflow are balanced. The volume is the integrated change in compartmental volume

$$\frac{dV}{dt} = \Phi_{\text{in}} - \Phi_{\text{out}} \quad V = \int \frac{dV}{dt}dt. \quad (7)$$

2) Anatomy of Heart Chambers and Valves: Throughout the model, all heart chambers are considered to be spherical in shape which should be tolerated in view of the intended applications. The inner radius changes with systole and diastole to host the atrial/ventricular momentary volume. Since the volume of each heart chamber's wall (the myocardium) is considered to be constant, the cavital wall thickens as the intracavital volume decreases in systole and thins in diastole when the ventricle fills. The resulting terms for radius and wall thickness are

$$r = \left(V_{\text{comp}}\frac{3}{4\pi}\right)^{1/3}$$
$$d = \left(V_{\text{wall}}\frac{3}{4\pi} + r^3\right)^{1/3} - r. \quad (8)$$

In (8), d [cm] is the wall thickness, r [cm] is the inner radius of the sphere (compartment), V_{comp} [l] is the volume inside the sphere, and V_{wall} [l] is the volume of the sphere's wall.

The calculation of the pressure inside the cardiac cavities is based on the Laplace law. This law relates wall tension, wall thickness, and pressure inside a hollow sphere by balancing the separating force with the product of wall tension and wall area as follows:

$$p = \sigma\frac{2dr + d^2}{r^2}. \quad (9)$$

In (9), σ [mm Hg] is the wall tension of the hollow sphere, d [cm] is the wall thickness, r [cm] is the inner radius, and p is the pressure inside.

The approach of modeling all heart chambers as hollow spheres is, of course, a simplification of reality. The left ventricle, for example, could be more accurately described as a spheroid [19]. This spheroid model would yield an about 25% lower wall tension than the spherical model for equal pressures and volumes [20]. However, during the course of systole, the left ventricle reshapes as a sphere. Since the wall tension is the driving input parameter to the model and, thus, not subject to interpretation, it can be adapted to the model geometry without affecting the validity of the simulation results.

Instead of suppressing negative flow values for mimicking the function of the heart valves, as is generally done, this model explicitly considers the heart valves. Fig. 3 shows the applied

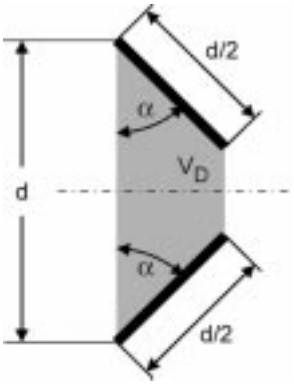

Fig. 3. Simplified modeling of cardiac valves. The shaded area is the dead space volume within the valves V_D.

geometry: the valvular opening angle determines the momentary dead space volume in the valves

$$V_D = D^3 \left(\frac{1}{2} \sin \alpha - \frac{1}{8} \sin 2\alpha \right). \tag{10}$$

In (10), V_D is the momentary dead space volume, D is the diameter of the valvular area, and α is the valvular opening angle.

Valvular closure is only complete (meaning that the flow is 0 l/min), when no blood is inside the valvular geometry (V_D is zero). This explicit mimicking of valvular function makes simulation of mild functional valve insufficiencies possible by means of choosing a large valvular geometry ($V_{D\max}$).

3) Simulation of Myocardial Processes: The heart cycle with systole and diastole is modeled by setting the appropriate wall tension for each moment in the heart cycle. Electrophysiology is not covered by this model, but could be included by a separate module.

The systolic change in the mechanical myocardial wall tension depends on the following components:

1) The two well-known effects of muscle physiology.
   - *Hill effect*: The instantaneous wall tension is negatively correlated with muscle cell shortening velocity.
   - *Frank-Starling effect*: maximal wall tension can be built up by a muscle cell with preload in the middle of the working range.
2) Inotropy, i. e., influences from the ANS.

High sympathetic activation raises the amplitude and speeds up the build-up of the maximum wall tension. Furthermore, it limits the influence of the Hill effect.

Both effects are incorporated in (11)

$$\sigma_{\text{prim}} = \begin{cases} \text{strength}_{\text{ventricle}} \times \text{auto}, & \text{systole} \\ 0, & \text{diastole} \end{cases}$$
$$\frac{d\sigma_{\text{pot}}}{dt} = \frac{\sigma_{\text{prim.}} - \sigma_{\text{pot}}}{Ca_{\text{const}}}. \tag{11}$$

In (11), σ_{prim} is the primary systolic wall tension without any delay, $\text{strength}_{\text{ventricle}}$ is a constant for the considered heart chamber representing the maximal force that the myocardium could generate under optimal preload with no afterload present (Table I), *auto* is the relative autonomic activity (value at rest: 1), σ_{pot} is the instantaneous potential wall tension without the Hill and Starling effects applied, and, finally, Ca_{const} is the integration constant describing the contraction and relaxation dynamics, respectively.

For the modeling of the Hill effect, the instantaneous myocardial shortening velocity is calculated from the first derivative of the ventricular/atrial circumference. This value is normalized by a linear transformation to a scalar of value from zero to one using a graphically derived Hill function curve. Since the importance of the Hill effect depends on inotropy [21], the slope of the Hill function curve is parametrized by varying the abscissa intersection according to autonomic activity through interpolation of the standard abscissa intersection and the abscissa intersection for maximal inotropy (both specific constants for each heart chamber), weighted by the value of the variable *auto* from (11).

For the implementation of the Frank-Starling effect, it is assumed that the inner radius of the heart chamber is proportionally related to the preload. This radius is transformed into a scalar (zero to one) using the Frank-Starling function curve.

The actual instantaneous wall tension σ is derived from σ_{pot} (11) by multiplying it with both factors from the Hill and Frank-Starling effects.

4) Parameters of the Model: Table I lists all scalar parameters used in the model equations. They are chosen to represent a mean healthy human subject. Discussion of the values and references is given as follows.

Cross sections of the heart valves: the values are taken from [22].

Volumes of myocardium: Left-ventricular wall volume is taken from [22, p. 98, table 11, NMR planimetry]. The other values are calculated from the respective masses [22, p. 67, table 11] by division by the assumed density of 1.04 g/ml [22, p. 98, table 11]. The septal volume was added to both ventricles, respectively.

Inertances: There is a wide range of values reported in the existing literature: in [8] the value for the aortic valve is given as $0.000\,061\,1$ mm Hg min^2/l, whereas [19] uses $0.000\,42$ mm Hg min^2/l. Using (2), an estimation based on the geometry is: assumed length of the accelerated column of fluid to be 10 cm. Mean cross section of this column (ventricle and outflow tract): 3.14 cm^2 (radius 1 cm). Density of blood: 1.05 kg/l. Using (2) gives

$$L_{\text{left ventr}} = 9.98 \cdot 10^{-6} \frac{\text{mm Hg min}^2}{l}. \tag{12}$$

Resistance to pulmonary blood flow: A meta-analysis of existing literature [22] (p. 72, tab.36) lists reference values from 0.8 to 1.4 mm Hg min 1^{-1}.

Dead space volumes of the heart valves: The chosen values are estimates derived from the geometrical assumptions (Fig. 3). These values influence the fraction of blood reflux in early diastole (10%–20% are normal for healthy subjects [24] and, thus, the depth of the aortic pressure dip [Fig. 5(a)].

Time constants for wall tension generation: Since, to the knowledge of the authors, no quantitative information has yet been published, the chosen values are derived from the dynamics of ventricular/atrial outflow since these depend

TABLE I
STANDARD PARAMETERS OF THE PULSATILE MODEL

Description	unit	systemic	pulmonary
maximal systolic ventricular wall tension	g $(min^2cm)^{-1}$	3.00	2.50
maximal systolic atrial wall tension	g $(min^2cm)^{-1}$	1.50	0.70
cross section of semilunar valves	cm^2	2.37	2.63
cross section of av-valves	cm^2	5.22	8.43
ventricular inflow inertance	mmHg min^2 l^{-1}	4.0e-06	2.0e-06
ventricular outflow inertance	mmHg min^2 l^{-1}	1.0e-05	7.0e-06
atrial inflow inertance	mmHg min^2 l^{-1}	2.0e-06	2.0e-06
resistance to flow in pulmonary artery → vein	mmHg min l^{-1}	-	1.01
resistance to flow in renal artery → vein	mmHg min l^{-1}	82.60	-
resistance to flow in muscle artery → vein	mmHg min l^{-1}	97.40	-
resistance to flow in aorta	mmHg min l^{-1}	0.0500	-
resistance to flow in systemic arteries → vein	mmHg min l^{-1}	34.71	-
atrioventricular resistance to flow	mmHg min l^{-1}	0.09	0.05
ventricular resistance to outflow	mmHg min l^{-1}	0.05	0.055
atrial resistance to inflow	mmHg min l^{-1}	0.05	0.04
volume of ventricular myocardium	l	0.18	0.10
volume of atrial myocardium	l	0.017	0.015
ventricular Hill parameter	cm s^{-1}	58.00	45.00
atrial Hill parameter	cm s^{-1}	90.00	90.00
unstressed venous volume	l	2.50	0.50
compliance of the venous system	l $mmHg^{-1}$	0.10	0.165
dead space of av-valves	l	0.0025	0.0025
dead space of semilunar valves	l	0.0020	0.0020
wall tension time constant for increase	min	0.0005	0.0020
wall tension time constant for decrease	min	0.0003	0.0003

on the time constants for wall tension generation. Ventricular compliance is modeled by means of graphically defined pressure-volume curves for passive filling. The pressure-volume curve for the right ventricle is taken from [25] and has been shown to be valid for rest and exercise. A wide range of human left ventricular-pressure-volume curves has been reported in the existing literature. This is most probably due to a lack of standardization of experimental conditions. The curve chosen for the model is the one from [26] since this one can be thought of being the median of all curves, and was successfully applied in former numerous applications of the Guyton model.

C. Coupling of the Models

The two models communicate via an interface in a way that first the pulsatile model computes one complete heart cycle, then the hemodynamic variables are averaged over the heart cycle and transferred to the Guyton model, which computes the complete status for this time step and returns control to the pulsatile model.

III. VALIDATION AND PLAUSIBILITY TESTS

Validations and plausibility tests [27] have to show that such a model can correctly predict phenomena and data describing healthy subjects, as well as those with cardiac deficiencies. Also, the dynamics of the simulated variables should reproduce the process known from the literature.

A. Steady-State

With the parameters given in Table I, simulated pressures (Fig. 4) and volumes (not shown) result in steady-states being compatible with reported experimental data. All simulated values are within the 95% confidence interval characterizing the distribution of pressures and volumes within the "healthy" population.

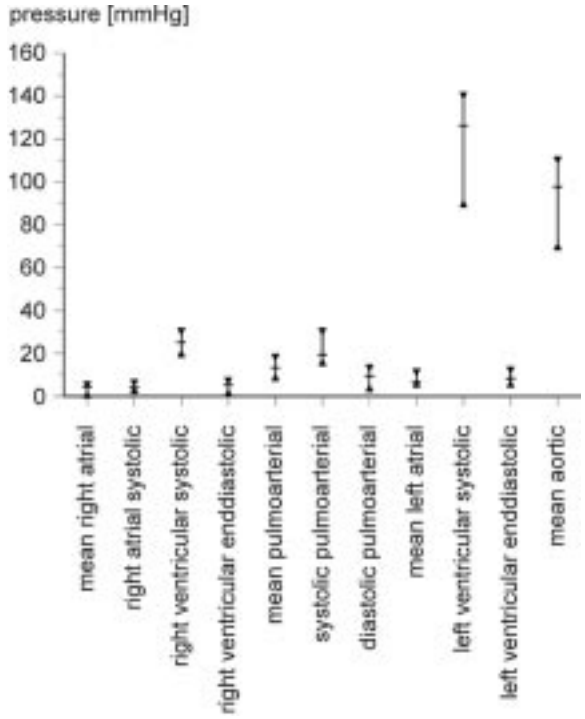

Fig. 4. Simulated steady-state values of 11 different pressures. Horizontal markers within the 95% confidence intervals in [23].

Since blood flow measurement is invasive, few quantitative data on blood flow in healthy subjects in the cardiovascular system have been published. Blood flow velocities on the other hand are well-known for various locations in the cardiovascular system of healthy subjects (Doppler ultrasound). Hence for the validation of simulated flow values these are transformed into the respective blood flow velocities using (13). This approach suffers from the problem that on the one hand the mean flow velocity is methodically hard to determine for a turbulent current and on the other hand the cross sectional area is hard to ascertain for complex anatomical locations. The real cross sectional area has often to be given as a simplified functional value. Furthermore these functional areas may change in the course of the heart cycle (pulmonary artery, [28]

$$\Phi = AV. \tag{13}$$

In (13), Φ [cm^3/s] is the flow, A [cm^2] is the cross-sectional area, and ν [cm/s] is the mean flow velocity. When taking the valve areas and the mean cross-sectional area of the ascending aorta as the cross-sectional areas A, also the calculated blood flow values are all within the 95% confidence intervals of experimental data.

1) Dynamics: The model reproduces the typical characteristics of the pressure curves of both heart chambers, pulmonary artery and aorta. The kink [Fig. 5(a)] in the ventricular pressure curves at around 430 ms (heart rate 70 min^{-1}) is due to the change from isovolumetric contraction to ejection phase and caused by the Hill effect. Simulated curves of pressure, wall thickness, wall tension and radius correspond to recorded ones.

When plotting the systolic and diastolic pressure values against the respective volumes, the resulting diagram is the characteristic pressure-volume loop [Fig. 5(b)]. The protuberance in the upper left of the loops is due to the blood reflux associated with the valvular closing processes. This principally physiolocial, but small deviation from an ideal p/V-diagram is generally not shown in physiology textbooks. Its distinctness in the simulation depends on the valvular parameters.

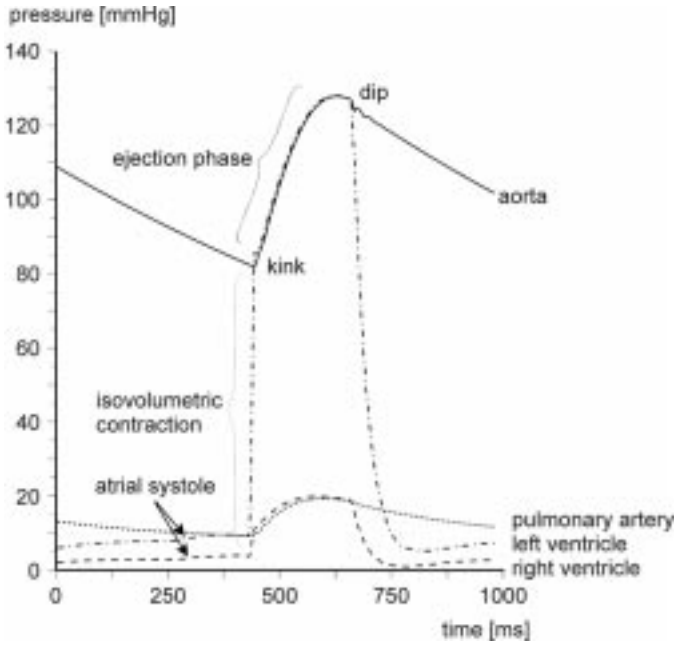

(a)

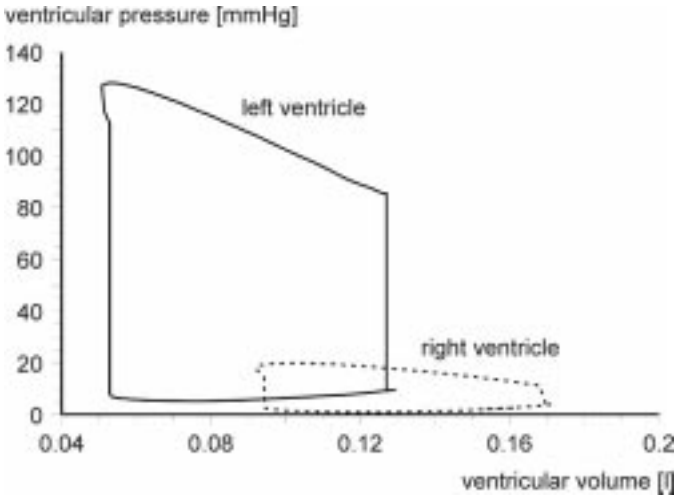

(b)

Fig. 5. (a) Simulated dynamics of pressures in both ventricles, in the aorta and in the pulmonary artery. Heart rate: 70 beats/min. (b) The simulated volume/pressure loop for the two ventricles.

The blood inflow velocity from the pulmonary veins into the left atrium has been investigated in [29]. The model simulates comparable flow curves. In Fig. 6(a) the flow component termed "J" is caused by ventricular contraction in systole and the flow phenomenon termed "K" is due to the early diastolic ventricular filling. Blood, thus, flows directly from the lungs into the left ventricle in early diastole. Simulated blood reflux into the lung is due to atrial contraction. For comparison of simulated to recorded data, the cross-sectional area was estimated as 10 cm^2, meaning a reasonable radius of around 0.9 cm per pulmonary vein.

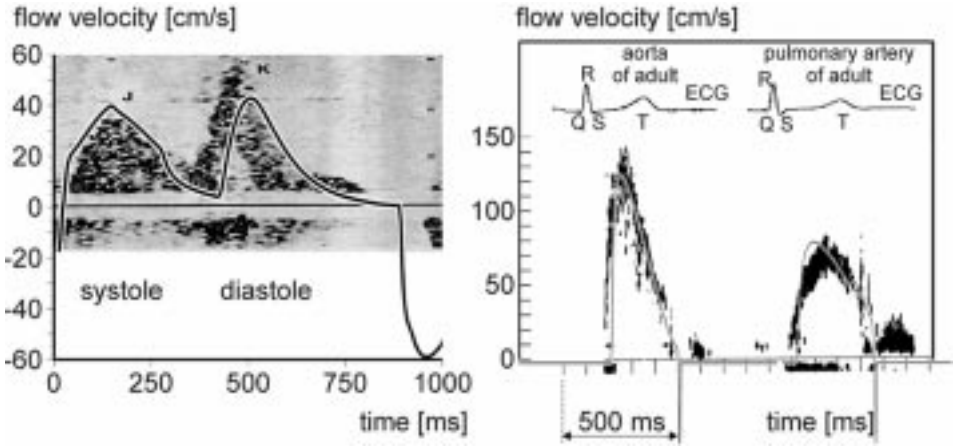

(a) (b)

Fig. 6. (a) Left-atrial inflow velocity. Line: simulation, signal: pulsed Doppler sonography from [29]. J = flow due to ventricular contraction in systole, K = early diastolic ventricular filling. (b) Pulmonary and aortic outflow. Line: simulation, signal: pulsed Doppler sonography from [22].

The ventricular outflow velocity was compared to recorded data as well [Fig. 6(b); the triangularly shaped left-ventricular outflow curve and the more smoothly configured right ventricular one are reproduced by the model]. The respective cross-sectional areas for conversion of flow into velocity values are those from Table I.

Fig. 7(a) and (b) presents simulation results of the well-understood pathophysiological phenomena of valvular deficiencies. Due to explicit modeling of the cardiac valves it is, e.g., possible to calculate the hemodynamics in aortic insufficiency [Fig. 7(a)]: simulation yields the expected phenomena such as high arterial pressure amplitude and low diastolic pressure due to early diastolic ventricular reflux.

Simulation of aortic stenosis [Fig. 7(b)] also yields plausible results: a high instantaneous ventriculoaortic pressure gradient, correlating to the degree of stenosis.

It has been reported [30] that a specific age-related change occurs in the left-ventricular volume curve over one heart cycle: the diastasis component of the ventricular volume curve (measurable by radionuclide ventriculography) which diminishes with age. Due to the high incidence of this condition, extensive focus has been given to simulation of various implications it may have on heart function. It is not only common to older healthy subjects in a mild form but also to patients suffering from many heart diseases such as hypertensive cardiopathy. First of all, the model confirms that the age dependency of the left-ventricular volume curve is most likely due to impaired myocardial relaxation in early diastole [Fig. 8(a)] Simulation of a relaxation disorder is achieved by increasing the time constant of the myocardial relaxation process from 18 ms to 54 ms.

The simulated normal influx into the left ventricle during the heart cycle is shown in Fig. 8(b), solid line. The two components are termed E and A, respectively, (in accordance with echocardiographic nomenclature). E is the early diastolic influx into the ventricle and A the influx attributable to atrial contraction. In the time interval between the two components there is very little ventricular inflow (diastasis). With a relaxation disorder simulated (broken line) the onset E of ventricular filling is delayed and reduced whereas the A component increases. This indicates the augmented importance of the atrial contribution when

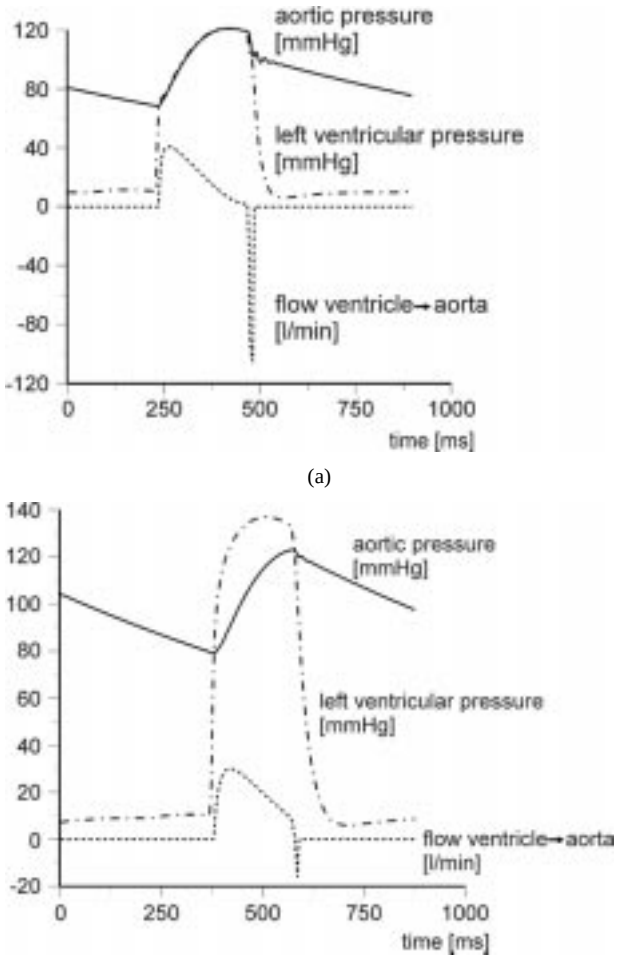

Fig. 7. (a) Simulation of aortic insufficiency by setting dead space volume of aortic valve V_D to 20 ml. (b) Simulation of aortic stenosis by increasing the left-ventricular outflow resistance from 0.05 mm Hgl/min to 1.3 mm Hgl/min. Heart rate: 70 beats/min.

ventricular relaxation is impaired, stressing, e.g., the hemodynamic benefits of dual-chamber pacing for that condition. Furthermore, the ventricular filling process then takes place in a shorter timeframe in diastole, meaning that with higher heart

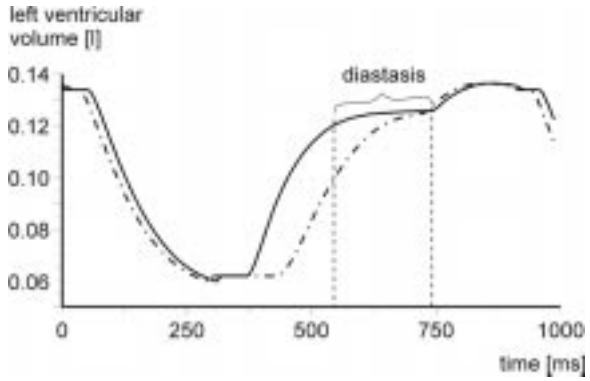

(a)

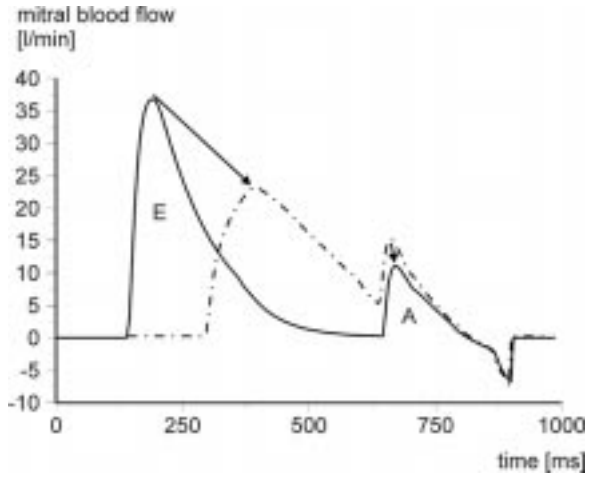

(b)

Fig. 8. (a) Simulated left-ventricular volume curve under normal conditions (unbroken line) and with impaired ventricular relaxation (broken line): The diastasis typical in young healthy subjects vanishes. (b) Mitral blood flow in normal state (unbroken line) and in patients with relaxation disorder (broken line). E = early inflow, A = inflow, due to atrial contraction.

rates (shorter diastole) there will not be enough diastolic time left for optimal ventricular filling.

At present it is not possible to use the coupled models for tests of long-term (days, weeks) phenomena, as the computing time on the available PCs is too excessive, which, however would be a very fruitful application because of the high performance of the Guyton model in this field (effects on kidney function, hormonal levels and chronic blood pressure levels).

IV. Application of the Model to Cardiac Electrotherapy

The influence of atrial synchronization and heart rate adaptation on the cardiopulmonary performance was investigated in detail by Lemke [31]. He examined patients suffering from chronotropic incompetence with implanted cardiac pacemakers. The criterion was the invasively measured central venous oxygen saturation S_{VO2} which, at a constant work load, strongly correlates with cardiac output. The coupled simulation system allows one to take into account the ergometer test protocol and the different modes of cardiac stimulation. Fig. 9 shows the results of the stimulation in comparison to Lemke's

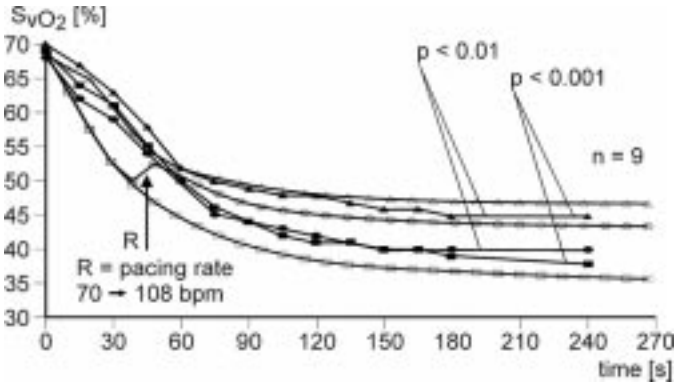

Fig. 9. Central venous oxygen saturation S_{VO2} in different pacing modes. Filled symbols: measurements in [31], open symbols: simulation. ■, □ VVI -, ▲, △ DDD-, •, ○ VVIR—Stimulation.

experimental results for ventricular sensing and stimulation inhibiting (VVI)-mode, VVI rate-adaptive (VVIR)-mode, and DDD-mode (atrial and/or ventricular, triggering, or inhibiting) stimulation. The calculated time constant and the delay of S_{VO2} correspond to values of the experimental study. To simulate VVI-stimulation we suppressed the systolic development of atrial wall tension and set heart rate to 70 beats-per-minute (beats/min). The superiority of DDD-stimulation versus VVI-stimulation is evident. In contrast to Lemke we found a difference between the effects of VVI- and VVIR-stimulation: Cardiac output at VVIR-stimulation in the simulation even turned out to be only insignificantly lower than at DDD-stimulation. We conclude that the patients in the Lemke-study did not profit hemodynamically from an increase of heart rate when there was no atrial contribution. The pacing rate (PR) of 108 beats/min chosen by Lemke at a work load of 50 W at VVIR-stimulation appears very high for a healthy proband and should according to the simulation compensate for the missing atrial contribution.

Sixty percent of the patients suffered from diseases which are accompanied by diastolic relaxation disorders (hypertrophy, coronary disease, cardiomyopathy). Therefore, we tested the model for predicting the effects of relaxation disorders on cardiac output. Indeed, simulation confirms that with relaxation impaired, stimulation above the adequate heart rate does not result in increased cardiac output [Fig. 10(a), broken lines], but in a substantial decrease, while healthy hearts do show some reserve. This is most obvious at rest. Hence impaired diastolic relaxation reduces tachycardia tolerance, stressing the need for an adjusted upper PR limitation.

Simulation data also support the thesis that with impaired myocardial relaxation the atrioventricular conduction time (AV-delay) has to be chosen carefully to get optimal cardiac output, whereas for healthy hearts a wide range of av-delays yield comparable pumping function [Fig. 10(b)], justifying the commonly fixed av-delay during DDD-pacing on patients without impaired diastolic function. Paced hearts with impaired myocardial relaxation though would benefit hemodynamically from an exercise dependent av-delay. Obviously this dependency of the cardiac output on the av-delay is due to the preload dependency of cardiac output (Frank-Starling mechanism). An algorithm for determining the optimal av-delay based on the first derivative of

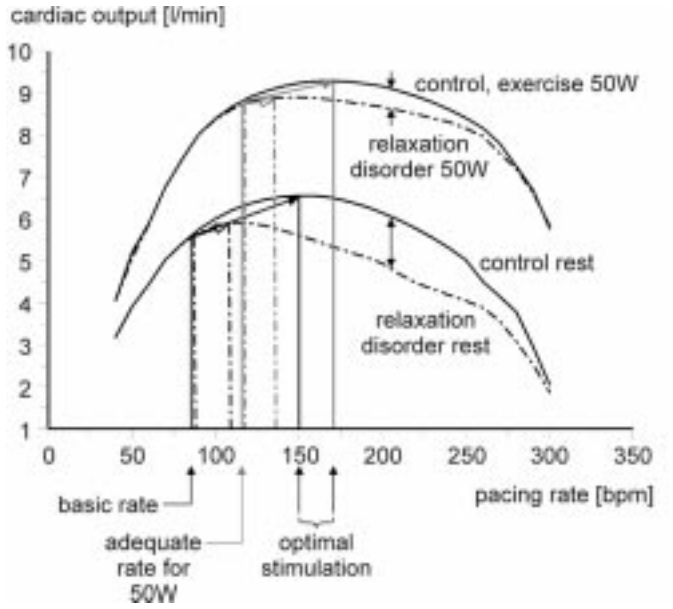

(a)

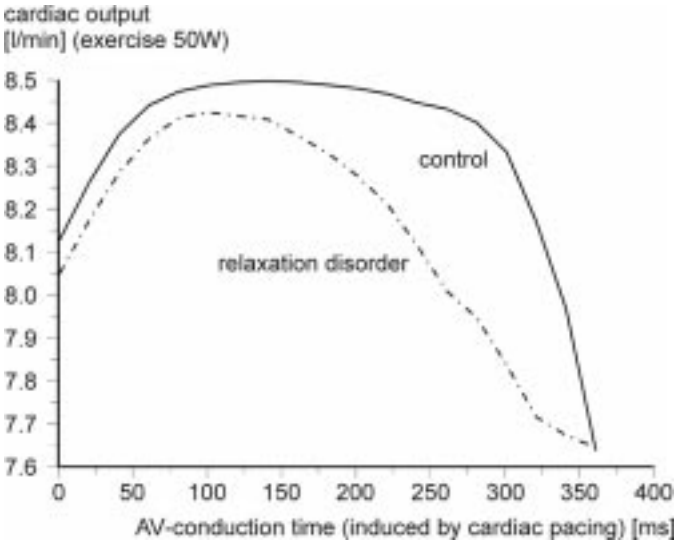

(b)

Fig. 10. (a) Simulated dependency of left-ventricular output on PR. In the status of relaxation disorder it is not possible to increase cardiac output by "overpacing" above the heart rate adequate to the exercise rate). (b) Simulated dependency of left-ventricular output on atrioventricular delay (as induced by cardiac pacing), influence of relaxation disorders.

the right-ventricular pressure (dependent on preload) was proposed for rest by [30]. This has been evaluated using this simulation results, which predicted acceptable results for normal hearts and for those with impaired myocardial relaxation even for exercise (treadmill) up to 100 W.

In rate adaptive pacing there are many requirements as to the choice of the parameter to be sensed. Historically a superior criterion has been good correlation with physical exercise. However, the primary question to be asked by the designer of a sensor-controlled pacemaker should be, how far the system restores the original physiological control-loop [32]. From this point of view, the most commonly implanted sensor-controlled pacemaker with an acceleration sensor in the pacemaker case is obsolete, as it does not reclose the physiological control-loop

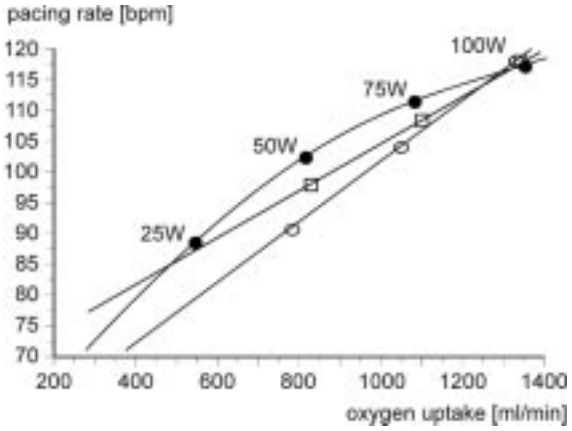

Fig. 11. Steady state relationship between oxygen uptake and PR in different types of sensor-controlled pacemakers. Sensor parameter: ◯ RMV, □ maximal right-ventricular pressure change, • central venous oxygen saturation.

and works independently of the actual physiological state. Therefore, in other pacemaker systems physiological parameters are sensed. Three of these (Fig. 11) central venous oxygen saturation S_{VO2}, respiratory minute volume (RMV), and maximal right-ventricular pressure $\mathrm{PEA}_{\max}$, were tested by simulation and compared as to their steady-state relationship between PR and oxygen uptake $\dot{V}_{\mathrm{O2}}$. The latter two systems show a linear relationship, mostly preferred by clinicians. However, from a technical standpoint, the nonlinear characteristic $\dot{V}_{\mathrm{O2}}$/PR could easily be compensated. It is interesting that the three systems deliver the same numerical relation at a work rate of 100 W, whereas at lower rates the system controlled by RMV requires lower PRs. However, we should like to point out that many other criteria determine the choice of the pacemaker.

V. Conclusion

The coupling of the two models turned out to be a promising tool for testing ideas and inspiring new studies and experiments in cardiology. The application of the program to cardiac electrotherapy done so far emphasizes the importance of atrial contraction to ventricular filling, the adequate ventricular delay, the effect of impaired ventricular relaxation, and the significance of the choice of the adequate cardiac pacemaker, both with respect to the stimulation site and the adequate sensor controlling PR. The program may also be useful for reproducing a consistent set of phenomena for educational purposes. The model system should be further improved to cover electrophysiological processes at the cellular level for studying pharmacodynamics and distribution of pharmacological agents, and to study long-term effects. Also further simulation studies for pathophysiological processes should be undertaken. However all simulated data have to be reviewed critically and require confirmation from other sources before final consequences for human treatment can result. The program will be distributed to everybody on request.

Acknowledgment

The authors express their deep gratitude to Dr. A. C. Guyton, Dr. T. G. Coleman, and Dr. J. P. Montani of the University of

Mississippi for providing their programs, experience, and advice.

REFERENCES

[1] N. Westerhof, F. Bosman, C. J. De Vries, and A. Noordergraaf, "Analog studies of the human systemic arterial tree," *J. Biomech.*, vol. 2, pp. 121–143, 1969.

[2] M. F. Snyder and V. C. Rideout, "Computer simulation of the venous circulation," *IEEE Trans. Biomed. Eng.*, vol. BME-16, pp. 325–334, 1969.

[3] A. C. Guyton, T. G. Coleman, and H. J. Granger, "Circulation: Overall regulation," *Ann. Rev. Physiol.*, pp. 13–43, 1972.

[4] G. Ferrari, C. De Lazzari, R. Mimmo, G. Tosti, and D. Ambrosi, "A modular numerical model of the cardiovascular system for studying and training in the field of cardiovascular physiopathology," *J. Biomed. Eng.*, vol. 14, pp. 91–107, 1992.

[5] G. Avanzolini, P. Barbini, A. Capello, and G. Cevenini, "CADCS simulation of the closed-loop cardiovascular system," *Int. J. Biomed. Comput.*, vol. 22, pp. 39–49, 1988.

[6] V. C. Rideout, "Cardiovascular system simulation in biomedical engineering education," *IEEE Trans. Biomed. Eng.*, vol. BME-19, pp. 101–107, 1972.

[7] K. Kampbell, M. Zeglen, and T. Kagchiro, "A pulsatile computer model for teaching heart-blood vessel interaction," *The Physiologist*, vol. 25, pp. 155–162, 1982.

[8] H. H. Hardy, R. E. Collins, and R. E. Calvert, "A digital model of the human circulatory system," *Med. Biol. Eng.*, vol. 30, pp. 550–564, 1982.

[9] H. Suga, "Theoretical analysis of a left-ventricular pumping model based on the systolic time-varying pressure-volume ratio," *IEEE Trans. Biomed. Eng.*, vol. BME-18, pp. 47–55, 1971.

[10] F. M. Melchior, R. S. Srinivasan, and J. B. Charles, "Mathematical modeling of human cardiovascular system for simulation of orthostatic response," *Amer. J. Physiol.*, vol. 262, pp. 1290–1333, 1992.

[11] C. W. Li and H. D. Cheng, "A nonlinear fluid model for pulmonary blood circulation," *J. Biomech.*, vol. 26, pp. 91–107, 1992.

[12] H. Tsuruta, T. Sato, M. Shirataka, and N. Ikeda, "Mathematical model of cardiovascular mechanics for diagnostic analysis and treatment of heart failure, Part 1. Model description and theoretical analysis," *Med. Biol. Eng. Comput.*, vol. 32, pp. 3–11, 1994.

[13] H. Tsuruta, T. Sato, and N. Ikeda, "Mathematical model of cardiovascular mechanics for diagnostic analysis and treatment of heart failure, Part 2. Analysis of vasodilator therapy and planning of optimal drug therapy," *Med. Biol. Eng. Comput.*, vol. 32, pp. 12–18, 1994.

[14] Y. Sun, B. J. Sjoberg, P. Ask, D. Loyd, and B. Wranne, "A mathematical model that characterizes transmitral and pulmonary venous flow velocity patterns," *Amer. J. Physiol.*, vol. 268, pp. H1476–H1489, 1995.

[15] M. Ursino, "Interaction between carotid baroregulation and the pulsating heart: A mathematical model," *Amer. J. Physiol.*, vol. 275, pp. H1733–H1747, 1998.

[16] A. C. Guyton, J. P. Montani, J. E. Hall, and R. D. Manning, Jr., "Computer models for designing hypertension experiments and studying concepts," *Amer. J. Med. Sci.*, vol. 295, pp. 320–326, 1988.

[17] J. P. Montani, T. H. Adair, R. L. Summers, T. G. Coleman, and A. C. Guyton, "A simulation support system for solving large physiological models on microcomputers," *Int. J. Biomed. Comput.*, vol. 24, pp. 41–54, 1989.

[18] A. C. Guyton, T. G. Coleman, and J. P. Montani, *Annotation of large circulatory model*, 1993.

[19] A. C. Guyton and C. E. Jones, *Cardiac Output and its Regulation*. Philadelphia, PA: Saunders, 1973.

[20] R. M. Huismann, P. Sipkund, N. Westerhof, and G. Elzinga, "Comparison of models used to calculate left ventricular wall force," *Med. Biol. Eng. Comput.*, vol. 18, pp. 133–144, 1980.

[21] E. Sonnenblick, E. Braunwald, and Williams, "Effects of exercise on myocardial force- velocity relations in intact unanesthetized man: Relative roles of changes in heart rate, sympathetic activity, and ventricular dimensions," *J. Clin. Investigat.*, vol. 44, pp. 2051–2062, 1965.

[22] C. Lentner, *Geigy Scientific Tables*. Nürnberg: Novartis Press, 1990, Heart and Circulation.

[23] H. Löllgen, *Kardiopulmonale Funktionsdiagnostik*. Basel, Switzerland: Ciba-Geigy, 1992.

[24] U. Sechtem, P. W. Pflugfelder, R. G. Gould, M. M. Cassidy, and C. B. Higgins, "Measurement of right and left ventricular volumes in healthy individuals with cine mr imaging," *Radiology*, vol. 3, pp. 697–702, 1987.

[25] K. R. Karsch and S. Scheufler, "The right ventricle at rest and during exercise," *Z. für Kardiol.*, vol. 7, pp. 485–490, 1979.

[26] A. C. Guyton, *Textbook of Medical Physiology*. Philadelphia, PA: Saunders, 1991.

[27] K. R. Godfrey, "Comments on parameter and structural identifiability concepts and ambiguities: A critical review and analysis," *Amer. J. Physiol.*, vol. 242, pp. 421–422, 1982.

[28] R. Paz, R. H. Mohiaddin, and D. B. Longmore, "Magnetic resonance assessement of the pulmonary arterial trunk anatomy, flow, pulsatility and distensibility," *Eur. Heart J.*, vol. 14, pp. 1524–1530, 1993.

[29] G. Keren, A. Bier, and J. Sherez, "Atrial contraction is an important determinant of pulmonary venous flow," *J. Amer. Coll. Cardiol*, vol. 7, pp. 693–695, 1986.

[30] R. Bauer, U. Busch, E. van der Flierdt, H. Stettmeier, W. Raab, H. R. Langhammer, and H. W. Pabst, "Altersabhängigkeit der herzfunktion bei herzgesunden," *Zeitschrift für Kardiologie*, vol. 77, pp. 632–641, 1988.

[31] B. Lemke, *Einfluß von Vorhofsynchronization und Frequenzsteigerung auf die Kardiopulmonale Leistungsfähigkeit und Neurohumerale Reaktion—Stellenwert der Frequenzvariablen Stimulation* Steinkopf, Darmstadt, 1997.

[32] J. Werner, M. Hexamer, M. Meine, and B. Lemke, "Restoration of cardio-circulatory regulation by rate-adaptive pacemaker systems: The bioengineering view of a clinical problem," *IEEE Trans. Biomed. Eng.*, vol. 46, pp. 1057–1064, Sept. 1999.

Jürgen Werner was born 1940 in Dortmund, Germany. He received the Dipl.-Ing. in electrical and control engineering and the Dr.-Ing. degrees from the Technical University of Darmstadt, in 1966 and1970.

In 1975, he became Professor of Physiology and in 1996 Professor of Biomedical Engineering at the Ruhr-University, Bochum, Germany. His main research interests comprise all problems of automatic control in medicine with special reference to the cardiovascular and the thermoregulatory system.

Daniel Böhringer was born 1972 in Marburg, Germany. He received the M.D. degree in 1999 from the Ruhr-University, Bochum, Germany.

He is currently working on simulation of cardiologic phenomena and cardiac pacing.

Martin Hexamer was born 1960. He received the Dipl.-Ing. degree in electrical engineering and the Ph.D. degrees from the Ruhr-University Bochum, Germany, in 1988 and 1994, respectively.

His main research topics are modeling and control and medical man-machine-systems.